Dispersion-free fiber transmission for femtosecond pulses by use of a dispersion-compensating fiber and a programmable pulse shaper

C.-C. Chang,* H. P. Sardesai,† and A. M. Weiner

School of Electrical and Computer Engineering, Purdue University, West Lafayette, Indiana 47907

Received September 22, 1997

We demonstrate nearly distortionless 2.5-km fiber transmission of sub-500-fs pulses, using a combination of standard single-mode fiber, dispersion-compensating fiber, and a programmable pulse shaper for simultaneous quadratic and cubic dispersion compensation. The dispersion-compensating fiber corrects the bulk of the quadratic and the cubic phases for the single-mode fiber, and the fiber-pigtailed programmable pulse shaper exactly compensates the residual dispersion terms. Together these elements permit complete recompression of pulses, which first broaden by ~400 times in the single-mode fiber. © 1998 Optical Society of America

OCIS codes: 260.2030, 320.2250, 320.0320, 060.0060.

Simultaneous compensation of quadratic, cubic, and higher-order dispersion is a key factor in the design of mode-locked lasers and chirped-pulse amplifiers operating at several tens of femtoseconds or less. The usual tools for compensating dispersion in such systems include grating pairs, prism sequences, and chirped dielectric mirrors, which are chosen to balance the quadratic and higher-order material dispersion. Transmission of femtosecond pulses over kilometer lengths of fiber is another application requiring simultaneous quadratic and cubic dispersion compensation.[1,2] We previously described the use of dispersion-compensating fiber (DCF) to compensate the quadratic dispersion and most of the cubic dispersion of standard single-mode fiber (SMF), permitting transmission of sub-500-fs pulses over several kilometers of fiber with only small distortion.[3] In this Letter we demonstrate for what is believed to be the first time the use of a programmable pulse shaper based on a liquid-crystal modulator array[4] as a programmable means for trimming the remaining cubic dispersion from this link, resulting in complete recovery of the original pulse.

We note that several other schemes, such as the use of dispersion-slope-compensating fiber,[5] chirped fiber Bragg gratings,[6] pulse shapers containing deformable mirrors,[7] and grating-and-lens pulse compressors set for nonzero dispersion,[2] were previously investigated for cubic dispersion compensation for subpicosecond-pulse fiber transmission. In the research reported in Ref. 8 a dispersion-equalizing fiber[8] was used that was capable of compensating not only the complete quadratic dispersion but also most of the cubic dispersion of SMF, and transmission of 62- and ~250-fs pulses over 42-m and 2.5-km DCF links, respectively,[1,3] was demonstrated. In both cases a small residual positive third-order dispersion remained that gave rise to some pulse broadening and oscillation in the tail of the output pulse. Here we employ a femtosecond pulse shaper containing a programmable liquid-crystal phase modulator (LCM) to compensate further the residual dispersion of the 2.5-km SMF–DCF link. As a result the residual dispersion is almost completely removed, and nearly dispersion-free 2.5-km fiber transmission for sub-500-fs pulses is obtained. Thus we use a fixed-fiber method for coarse dispersion compensation together with the LCM apparatus for fine tuning of the residual dispersion. In contrast with other schemes for dispersion-slope compensation, our programmable pulse-shaper approach can easily provide tunable fine tuning of the cubic phase alone (as well as potentially higher-order terms) without needing any mechanical adjustment.

Figure 1 shows a schematic diagram of our experimental setup. The 1.56-μm 65-fs pulses generated at ~30 MHz from a mode-locked Er-fiber ring laser are spectrally tailored (by an interference bandpass filter) and then amplified (by an Er-doped fiber amplifier), resulting in ~450-fs pulses of 1.2-mW average power. Note that our technique described below should also be applicable even to extremely high-repetition-rate systems, provided that the average power levels are not excessive. We inserted a low-loss (5.3-dB insertion loss), fiber-pigtailed femtosecond pulse shaper with a LCM (Ref. 4) into the Fourier plane before the 2.5-km transmission fiber link to provide fine tuning of the phase correction. Since the pulse shaper contains polarization-dependent elements, such as gratings and a LCM, we use a polarization controller on the input fiber pigtail to adjust the polarization state for the best power throughput. The LCM (supplied by Cambridge Research and Instrumentation) contains 128 phase-modulating pixels on 100-μm centers with ~3-μm interpixel gaps. Each pixel can be independently programmed to provide any gray-scale phase modulation from 0 to 3.5π. The phase function applied to a LCM can be reconfigured in a duration of millisec-

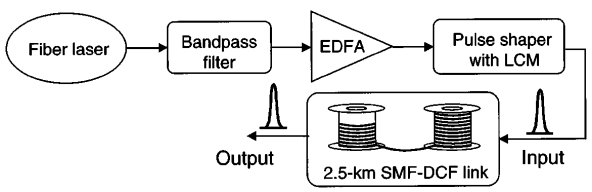

Fig. 1. Block diagram for the dispersion-compensation experiments. EDFA, Er-doped fiber amplifier.

0146-9592/98/040283-03$10.00/0

onds. The pulse shaper contains a pair of gratings (1100 lines/mm) and lenses (focal length, 19 cm) that are arranged to have a spatial dispersion ($\Delta x/\Delta\lambda$) of 0.71 mm/nm in the Fourier plane. The pulse shaper is adjusted to be in a minimum-dispersion configuration such that when 0 phase (or any arbitrary constant phase) is applied to all pixels of the LCM, the pulses are at their shortest possible width right at the output fiber end of the pulse shaper. The SMF after the pulse shaper acts as a spatial filter that removes any space–time coupling effects resulting from the pulse-shaping process.[9] Figure 2(a) shows the intensity cross-correlation trace of the pulses at the output port of the pulse shaper with constant phase applied, as measured by second-harmonic generation with the original 65-fs pulses as a reference. The output pulses broadened to a duration of ~480 fs FWHM owing to modest spectral narrowing, which was apparently associated with a spectral dependence of the input polarization state coupled with the polarizing properties of the grating. Theses pulses are input into a 2.5-km SMF–DCF link that consists of 2060 m of SMF (AT&T 5D) and 445 m of DCF (AT&T JRFDC1074C1DC) and is dispersion optimized by adjustment of the length ratio of the SMF and the DCF. The pulses would broaden to ~200 ps after propagating over 2060 m of SMF, and the subsequent 445-m DCF compensates most of the dispersion in SMF and recompresses the pulses to ~580 fs, as shown in the cross-correlation trace (with the original 65-fs pulses as a reference) in Fig. 2(b). The output pulses show small oscillation in the tail, indicating small residual positive third-order dispersion, as observed earlier.[1–3]

To compensate further for this residual dispersion slope, we applied a cubic-phase variation across the LCM. Using our earlier estimation of the dispersion slope of the SMF–DCF link[3] as a starting point, we iteratively adjusted the amount of cubic phase applied to LCM to remove completely the oscillation in the pulse tail. Figure 2(c) shows the cross correlation of the output pulse from the 2.5-km link when an optimal positive cubic phase [Fig. 2(d)] was applied. The quadratic and the cubic phases provided by pixel n of the LCM can be formulated as

$$\Phi_n = \frac{\phi_2}{2}(n - 64)^2\delta\omega^2 + \frac{\phi_3}{6}(n - 64)^3\delta\omega^3, \qquad (1)$$

where $n = 1, 2, 3, \ldots, 128$; ϕ_2 (in squared picoseconds) and ϕ_3 (in cubic picoseconds) are the second- and third-order phase dispersion, respectively; and $\delta\omega$ is the angular frequency increment (which is 1.1×10^{11} rad/s in our case) between adjacent pixels. The phase variation is discretely sampled over the entire 128 pixels, but since the phase difference between the first and the last pixel is quite small ($\sim 2.1\pi$), the variation can basically be considered continuous sampling. Therefore exact phase correction is feasible, as one can see from Fig. 2(c), such that the small cubic phase is compensated and the pulse (of ~490 s) is almost restored to the input pulse width. The optimal applied cubic phase in Fig. 2(d) corresponds to a third-order dispersion ϕ_3 of 0.06 ps^3. Since the phase accumulated after passing through fiber of length L can be expressed as

$$\Phi_F(\omega) = -\frac{\beta_2}{2}(\omega - \omega_0)^2 L - \frac{\beta_3}{6}(\omega - \omega_0)^3 L + \ldots, \qquad (2)$$

the residual third-order dispersion coefficient β_3 of the 2.5-km dispersion-compenstated SMF–DCF link is +0.024 (±0.006) ps^3/km. This number is four or five times less than that of dispersion-shifted fiber (DSF) and is roughly consistent with our earlier measurement of a 42-m fiber link (+0.018 ps^3/km) by use of spectral interferometry.[3] Note that, although the phase curve in Fig. 2(d) ranges from $\sim 1.1\pi$ to $\sim 1.0\pi$, in reality the phase applied to each pixel is π to 3π modulo 2π.

To demonstrate the ability to program the magnitude and the sign of the cubic-phase term, in Figs. 3(a) and 3(b) we show the intensity profiles of the output pulses from the 2.5-km fiber link when cubic-phase variations ϕ_3 of −0.25 and +0.25 ps^3, respectively, are applied to the LCM. The larger applied cubic phases clearly result in more-pronounced oscillating tails in the time-domain data. By choosing the sign of the cubic phase we can select the oscillatory tail either before or after the main pulse. Note that the oscillation shown in Fig. 3(a) is more pronounced than that in Fig. 3(b) because the total amount of cubic phase in Fig. 3(a) (−0.31 ps^3, including the SMF–DCF link) is larger than in Fig. 3(b) (+0.19 ps^3, including the SMF–DCF link).

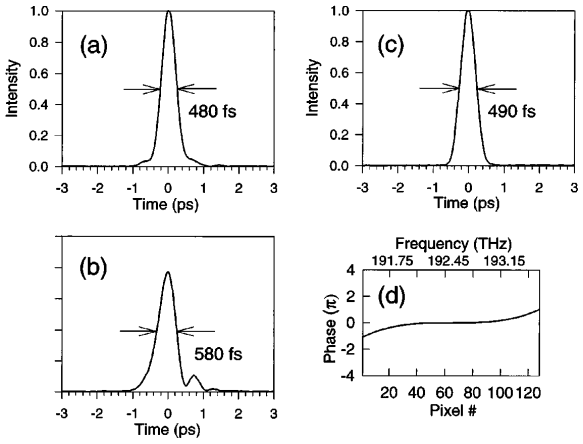

Fig. 2. Input pulse to (a) the 2.5-km fiber link and output pulse from the fiber link when (b) constant-phase or (c) cubic-phase correction is applied to the LCM. (d) Cubic-phase-correction function.

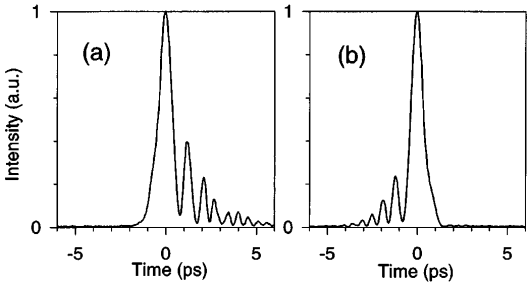

Fig. 3. Intensity cross-correlation measurements of the output pulses from the 2.5-km SMF–DCF link when a cubic phase of (a) −0.25 ps^3 (total, −0.31 ps^3) or (b) +0.25 ps^3 (total +0.19 ps^3) is applied to the LCM.

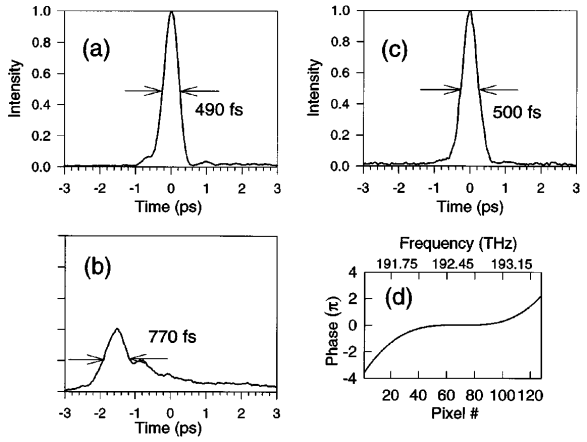

Fig. 4. (a) Input pulse to the 3-km SMF–DCF–DSF fiber link and (b) output pulse from the fiber link when constant-phase or (c) cubic- and quadratic-phase correction is applied to the LCM. (d) Phase-correction function.

Although the dispersion-free transmission length of 2.5 km demonstrated here is already suitable for local-area-networking applications such as femtosecond-pulse code-division multiple access,[10] we did not reach the phase-modulation capacity of the LCM. To test our LCM for higher cubic-phase compensation, we added a 500-m DSF that has zero dispersion wavelength (1559 nm) close to the center wavelength (~1558 nm) of our pulses. Figures 4(a) and 4(b) show the intensity cross correlations of the input pulses (FWHM, ~490 fs) and the output pulses (FWHM ~770 fs), respectively, of the 3-km SMF–DCF–DSF link when no phase correction is applied to the LCM. As demonstrated in Fig. 4(b), the added 500-m DSF transmission results in more-negative cubic-phase variation (ϕ_3), indicated by the more-pronounced tail as well as some quadratic phase that partially washes out the oscillation in the tail. By applying a cubic-phase compensation ϕ_3 of 0.125 ps^3 and a small quadratic-phase correction ϕ_2 of 0.05 ps^2 [Fig. 4(d)], we were able to compress the pulses to 500 fs, almost the original pulse width, as shown in Fig. 4(c).

We briefly discuss the maximum dispersion-compensation capacity of our setup. When the pulse shaper has sufficient spectral resolution, the dispersion is limited by the requirement that the maximum phase shift from one modulator pixel to the next remain less than $\pi/2$, so the discrete array adequately samples the desired phase function. For the cubic spectral phase, this requirement implies that[4]

$$|\phi_3| < \frac{4\pi}{N^2 \delta\omega^3}, \tag{3}$$

where N is the number of pixels in the array. For our parameters, $|\phi_3| < 0.58$ ps^3. Focusing the individual frequency components to spots larger than individual pixels, as in the current experiments, reduces the spectral resolution and restricts the available time window for pulse shaping.[9,11] Our current spectral resolution is ~0.02 THz (0.16 nm), which corresponds to ~1.3 pixels. This resolution results in a time window for pulse shaping $|t| < 11$ ps, which implies that $|\phi_3| < 0.45$ ps^3. The spectral resolution, time window, and maximum cubic phase can be adjusted through choice of the pulse shaper and the incoming pulse parameters.

In conclusion, we have demonstrated nearly distortionless linear transmission of sub-500-fs pulses over 2.5 km of a SMF–DCF link and 3 km of a SMF–DCF–DSF link, using a combination of a DCF and a LCM. We also believe that a transmission distance a few times longer (>10 km) is possible if the combined techniques of DCF and LCM are exploited to their full capacity. With a low insertion loss and fiber pigtails at both ends, our pulse shaper with a LCM can also be integrated with other fiber-optic components for spectral phase filtering, waveform synthesis, and higher-order dispersion compensation. In addition, our experiments give a clear demonstration of the phase-correction capabilities made possible by programmable femtosecond pulse shapers, which can potentially be applied for higher-order compensation in other systems, such as chirped-pulse amplifiers.

We acknowledge support from the National Science Foundation under grants ECS-9312256 and ECS-9626967. We thank A. M. Vengsarkar and D. W. Peckham for the DCF and SMF fibers used in the dispersion-compensation experiments and M. Newhouse and V. Da Silva for the Er fiber and the DSF.

*Present address, Bell Labs, Lucent Technology, Holmdel, New Jersey, 07733.

†Present address, Ciena Corporation, 920 Elkridge Landing, Linthicum, Maryland 21090.

References

1. C.-C. Chang, A. M. Weiner, A. M. Vengsarkar, and D. W. Peckham, Opt. Lett. **21,** 1141 (1996).
2. M. Stern, J. P. Heritage, and E. W. Chase, IEEE J. Quantum Electron. **28,** 2742 (1992).
3. C.-C. Chang and A. M. Weiner, IEEE J. Quantum Electron. **33,** 1455 (1997).
4. A. M. Weiner, D. E. Leaird, J. S. Patel, and J. R. Wullert II, IEEE J. Quantum Electron. **28,** 908 (1992).
5. S. Kawanishi, H. Takara, T. Morioka, O. Kamatani, K. Kikoh, and M. Saruwatari, Electron. Lett. **9,** 457 (1996).
6. L. Dong, M. J. Cole, A. D. Ellis, M. Durkin, M. Ibsen, V. Gusmeroli, and R. I. Laming, in *Optical Fiber Communication Conference*, Vol. 6 of 1997 OSA Technical Digest Series (Optical Society of America, Washington, D.C., 1997), p. 391.
7. J. P. Heritage, E. W. Chase, R. N. Thurston, and M. Stern, in *Conference on Lasers and Electro-Optics*, Vol. 10 of 1991 OSA Technical Digest Series (Optical Society of America, Washington, D.C., 1991), p. 74.
8. A. M. Vengsarkar, A. E. Miller, M. Haner, A. H. Gnauck, W. A. Reed, and K. L. Walker, in *Optical Fiber Communication Conference*, Vol. 4 of 1994 OSA Technical Digest Series (Optical Society of America, Washington, D.C., 1994), p. 225.
9. R. N. Thurston, J. P. Heritage, A. M. Weiner, and W. J. Tomlinson, IEEE J. Quantum Electron. **22,** 682 (1986).
10. J. A. Salehi, A. M. Weiner, and J. P. Heritage, IEEE J. Lightwave Technol. **8,** 478 (1990).
11. A. M. Weiner, Progr. Quantum Electron. **19,** 161 (1995).